Molecular and Cellular Biomedical Sciences, Vol.10 No.1, March 2026, p. 1-70
Print ISSN: 2527-4384, Online ISSN: 2527-3442
DOI: 10.21705/mcbs.v10n1.751

RESEARCH ARTICLE

MCBS
Mol Cell Biomed Sci. 2026; 10(1): 42-54
DOI: 10.21705/mcbs.v10n1.751

Dual Target Anticancer Potential of *Exiguobacterium*-derived Metabolites from the Maros-Pangkep Karst: An *In Silico* Study Targeting EGFR and Caspase-3

Taswin Wijaya[1], Nur Haedar[1], Helmy Widyastuti[1], Riuh Wardhani[1,2], Fuad Gani[1]

[1]*Department of Biology, Faculty of Mathematics and Natural Sciences, Universitas Hasanuddin, Makassar, Indonesia*
[2]*Division of Animal and Dairy Science, Chungnam Natioanl University, Daejon,Republic of Korea*

Background: Cancer is the second leading cause of death worldwide and its multifactorial nature limits the effectiveness of single-target therapies. Combination treatments may improve efficacy but are often associated with toxicity and drug interactions. Extremophilic bacteria from karst environments remain underexplored as sources of multitarget anticancer compounds. This study aimed to evaluate the dual-target anticancer potential of bioactive metabolites produced by bacteria isolated from the Maros–Pangkep karst region using molecular docking and ADME analysis.

Materials and methods: A bacterial isolate obtained from soil samples from the Maros–Pangkep karst region, Indonesia, was selected based on colony morphology and identified as *Exiguobacterium* using 16S rRNA gene analysis. Bioactive compounds were characterized by GC-MS, and three major metabolites were docked against EGFR (PDB ID: 1M17) and caspase-3 (PDB ID: 1PAU). ADME analysis was performed to evaluate drug-likeness and toxicity.

Results: Docking analysis showed that compound (1) Pyrrolo[1,2-a]pyrazine-1,4-dione, hexahydro-3-(2-methylpropyl) exhibited the strongest binding affinity toward EGFR (−7.2 kcal/mol), exceeding the native ligand erlotinib (−6.1 kcal/mol). Compound (2) Cyclo(L-prolyl-L-valine) and compound (3) 2,5-piperazinedione,3-methyl-6-(1-methylethyl) derivatives showed binding affinities of −6.4 and −5.9 kcal/mol, respectively. For caspase-3, the compounds displayed binding affinities ranging from −4.5 to −6.0 kcal/mol , exceeding the native ligand Ac-DEVD-CHO (−3.6 kcal/mol) and interacted outside the active site, indicating potential allosteric activation. All compounds complied with Lipinski's rule of five and showed low toxicity (LD50>800 mg/kg).

Conclusion: This study shows that metabolites from *Exiguobacterium* possess dual-target anticancer potential via EGFR inhibition and caspase-3 modulation, suggesting their use as multitarget drug candidates.

Keywords: *16S rRNA, bacteria, biological products, caspase-3, epidermal growth factor receptor, Kart Maros-Pangkep, molecular docking*

Submission: November 9, 2025
Last Revision: December 26, 2025
Accepted for Publication: January 05, 2026

Corresponding Author:
Nur Haedar
Department of Biology, Faculty of Mathematics and Natural Sciences
Universitas Hasanuddin
Jl. Perintis Kemerdekaan KM 10, Makassar 90245, Indonesia
e-mail: nurhaedar@unhas.ac.id

Introduction

Cancer is the second leading cause of death worldwide after cardiovascular disease, with global mortality expected to continue rising in the coming decades.[1] The epidermal growth factor receptor (EGFR), also known as ErbB1 or HER1, is a receptor tyrosine kinase that regulates cell proliferation, survival, and differentiation. Aberrant activation or overexpression of EGFR is closely associated with the development and progression of various cancers, including lung, breast, colorectal, and pancreatic cancers. Consequently, EGFR has become an important molecular target in anticancer therapy.[2]

Despite their clinical use, EGFR inhibitors often exhibit limited efficacy due to tumor heterogeneity, mutation-specific responsiveness, and the emergence of drug resistance. Moreover, cancer is a multifactorial disease involving multiple interconnected signaling pathways, making single-target therapies prone to treatment failure. Although combination therapies have shown improved outcomes, their clinical application remains challenging because of increased toxicity, drug–drug interactions, and complex pharmacokinetics. As an alternative strategy, multitarget or dual-target agents capable of modulating multiple cancer-related pathways with a single molecule have gained increasing attention due to their potential for improved efficacy and reduced side effects.[3]

Cancer progression is governed by the interplay between proliferation and apoptosis pathways. EGFR activation stimulates the PI3K/AKT signaling cascade, promoting cell survival and suppressing apoptotic signaling, including the inhibition of caspase activation. In contrast, caspase-3 is a key executioner protease responsible for the cleavage of essential cellular substrates during programmed cell death. Simultaneous modulation of EGFR mediated proliferation and caspase-3 dependent apoptosis therefore represents a promising dual-target strategy for anticancer drug development.[4-6]

The urgent need for novel anticancer agents has intensified the exploration of microorganisms as sources of bioactive secondary metabolites. Extremophilic environments, such as karst ecosystems, are characterized by unique physicochemical conditions, including mineral-rich substrates, variable pH, and fluctuating humidity, which can drive microbial metabolic diversity. The Maros-Pangkep karst region in South Sulawesi, Indonesia, represents one of the largest tropical karst landscapes and remains largely unexplored for its microbial biodiversity and chemical potential.[7] Microorganisms inhabiting this environment are therefore expected to produce structurally distinct metabolites with unique biological activities.

However, there is currently no systematic evidence regarding the multitarget anticancer potential of bacterial metabolites derived from karst ecosystems, particularly with respect to simultaneous modulation of EGFR and apoptosis-related pathways such as caspase-3. Accordingly, this study aimed to identify major bacterial metabolites from the Maros-Pangkep karst region and evaluate their potential as dual-target anticancer agents using molecular docking and computational analyses.

Materials and methods

Bacterial Isolation

Bacterial isolation was performed from soil samples collected from the Maros–Pangkep karst region, South Sulawesi, Indonesia. Approximately 5 g of each soil sample was suspended in 45 mL of aquadest and homogenized by vortexing for 2 minutes. Serial dilutions (10^{-1} to 10^{-6}) were prepared, and 100 µL aliquots from appropriate dilutions were spread onto solid Nutrient Agar (NA; Oxoid™, Cat. No. CM0003; Thermo Fisher Scientific, Basingstoke, UK) plates using sterile glass spreaders. Plates were incubated at 37°C for 24 hours. Isolate selection was based on differences in colony morphology, including shape, color, margin, and surface texture, to obtain microbial diversity. Isolates with contrasting morphologies were purified by repeated streaking on NA plates until pure cultures were obtained. Isolates with distinct and contrasting morphologies were selected for further development without initial screening for biological activity. This approach was commonly employed in microbial bioprospecting studies from extreme environments, as variations in colony morphology often reflected differences in the secondary metabolites produced.[8-9]

Phenotypic Characterization

Bacterial strains were identified to the genus level based on colony morphology (shape, elevation, edge, and color), microscopic examination (Gram staining, endospores, and cell shape), biochemical tests (motility, indole, Hydrogen Sulfide (H_2S), sugar and gas (Triple Sugar Iron Agar

Print ISSN: 2527-4384, Online ISSN: 2527-3442
DOI: 10.21705/mcbs.v10n1.751

test), Methyl Red-Voges Proskauer (MR-VP), citrate, and catalase) using standard procedures.[10-14] Strains were coded and numbered from B-1 to B-6.

Bioactive Compound Analysis

The identification of antibacterial compounds was conducted using Gas Chromatography–Mass Spectrometry (GC-MS). The selected bacterial isolate was cultured in Mueller Hinton Broth (MHB) medium (Oxoid™, Cat. No. CM0405; Thermo Fisher Scientific, Basingstoke, UK) for 3 days using a shaker (IKA KS 260 Basic, Germany), then centrifuged (Eppendorf 5702, Germany) to obtain a cell-free supernatant. The supernatant was extracted with ethyl acetate (Merck, Cat. No. 822277; Darmstadt, Germany) in a 1:1 ratio using a separatory funnel. The ethyl acetate layer was separated and evaporated using a rotary evaporator (Heidolph Laborota 4000, Germany) at 70°C for 40 minutes to obtain a concentrated extract.[15] GC-MS analysis of the concentrated ethyl acetate extract was carried out using an Operating GC-MS Ultra QP 2010 Shimadzu (Shimadzu Corp, Japan).[16] One hundred microliters of the concentrated extract were injected into the chromatography column. The injector temperature was set at 250°C in splitless mode, with a pressure of 76.9 kPa, a flow rate of 14 mL/min, and a split ratio of 1:10. The ion source and interface temperatures were 200°C and 280°C, respectively, with a solvent cut time of 3 minutes and mass scan range of 40–700 m/z. The column used was SH-Rxi-5Sil MS, 30 m in length with an internal diameter of 0.25 mm. The initial column temperature was set at 70°C with a hold time of 2 minutes, increased to 200°C at a rate of 10°C/min, and then to 280°C with a final hold time of 9 minutes at a rate of 50°C/min, resulting in a total run time of 36 minutes. The resulting chromatogram data were analyzed using the NIST 17 and Wiley 9 spectral libraries.

Molecular Docking Analysis

The biological activity of the compounds identified through GC-MS analysis was evaluated using molecular docking techniques. Compound identification numbers were retrieved from the PubChem database (https://pubchem.ncbi.nlm.nih.gov/), and their three-dimensional (3D) structures were downloaded in SDF format and converted to PDB format using AutoDockTools v1.5.7. The structure of these compounds includes: Cyclo(L-prolyl-L-valine) (PubChem CID: 6992261), Pyrrolo[1,2-a]pyrazine-1,4-dione,hexahydro-3-(2-methylpropyl)(PubChem CID: 7074739), and 2,5-Piperazinedione,3-methyl-6-(1-methylethyl) (PubChem CID: 139895). To predict potential protein targets, a literature review was conducted, focusing on commonly studied anticancer target proteins. The selected targets were validated using UniProt (https://www.uniprot.org).[17] The protein structures of EGFR (PDB ID: 1M17, resolution: 1.62 Å) and caspase-3 (PDB ID: 1PAU, resolution: 1.50 Å) were obtained from the Protein Data Bank (https://www.rcsb.org/). Protein structures were prepared by removing water molecules, adding polar hydrogens, and assigning Kollman charges using Chimera v1.17.3 and AutoDockTools v1.5.7.18 Grid box coordinates were defined based on the native ligand position with dimensions of 60×60×60 points and a spacing of 0.375 Å, centered on the native ligand. Docking was performed using PyRx v0.8 with the AutoDock Vina engine. Each ligand was docked in triplicate. The mean binding affinity was calculated to evaluate docking consistency, while the lowest-affinity conformation was selected for interaction analysis. Redocking of the native ligand was performed to validate the docking protocol. Docking results were visualized using PyMOL v2.5 and Biovia Discovery Studio Visualizer v21.1 to analyze hydrogen bonds, hydrophobic interactions, and other ligand–protein contacts.[19]

Drug-likeness Evaluation of Test Ligands

The solubility characteristics and structural descriptors of the selected ligands were analyzed using the web-based platform SwissADME.[20] Compliance with Lipinski's rule was evaluated based on log P values, molecular weight, and the number of hydrogen bond donors and acceptors. Additionally, adherence to Veber's rule was assessed by calculating the topological polar surface area (TPSA) of compound (1) Cyclo(L-prolyl-L-valine), compound (2)pyrrolo[1,2-a]pyrazine-1,4-dione,hexahydro-3-(2-methylpropyl), and compound (3) 2,5-piperazinedione,3-methyl-6-(1-methylethyl). The toxicity profiles of the designed compounds were predicted using the open-source online tool ProTox-II (http://tox.charite.de/protox_II) by estimating their median lethal dose (LD50) values.

Identification of Bacterial Isolates using 16S rRNA Gene Sequencing

To accurately identify bacterial isolates at the species level, a DNA-based molecular approach was employed.[21] DNA was

performed using the Geneaid Presto™ Mini gDNA Bacteria kit (Geneaid Presto™, Taipei, Taiwan) with a special procedure for Gram-positive bacteria. Cells underwent enzymatic and chemical lysis, followed by purification through a spin column until pure DNA extract was obtained. 16S rRNA gene amplification was performed using PCR with universal primers 63F (5'- CAGGCCTAACACATGCAAGTC-3') and 1387R (5'- GGGGGGTGTGTACAAGGC-3'). PCR amplification was carried out in a total volume of 25 µL containing 12.5 µL of 2× Master Mix, 1 µL of each primer (10 µM), 2 µL of template DNA, and nuclease-free water. The reaction was performed under the following thermal conditions: initial denaturation at 95°C for 5 min; 35 cycles of denaturation at 95°C for 30 s, annealing at 55°C for 30 s, and extension at 72°C for 1 min; followed by a final extension at 72°C for 10 min. PCR visualization was performed using 1.5% agarose gel electrophoresis with ethidium bromide. The product was considered positive if a DNA band of approximately ~1500 bp was observed. DNA sequencing was performed on positive PCR products. The sequence results were analyzed using Basic Local Alignment Search Tool (BLAST) against the National Center for Biotechnology Information (NCBI) database to identify bacterial species based on 16S rRNA gene sequence similarity.[22]

Results

Isolation of Bacteria Based on Morphology and Phenotypic Characterization

A total of 6 bacterial strains were obtained from the Maros-Pangkep karst region. Isolates were selected based on their unique morphological characteristics to maximize the diversity of metabolites potentially produced by the microorganisms.[23] The selected colony isolate with code B-6 had a unique morphology, as determined by morphological observations (Figure 1 and Table 1). This morphology differed from the morphology of other strains. Microscopic examination revealed that the selected isolate, B-6, was gram-positive, short rod-shaped, and does not form endospores. The colony was large, grew rapidly, and had an irregular shape with a flat elevation, curled edges, and a beige color. The isolate tested positive for motility, the TSIA sugar test, MR-VP, and catalase. The phenotypic characteristics of the other isolates were shown in Table 2.[24]

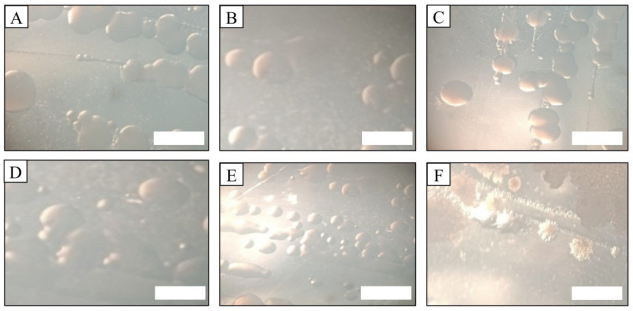

Figure 1. Morphological observation results of bacterial isolate colonies. A: B-1 isolate; B: B-2 isolate; C: B-3 isolate, D: B-4 isolate; E: B-5 isolate; F: B-6 isolate. White bar: 30x magnification.

Compound Analysis using GC-MS

The fermentation and extraction results of the selected isolates yielded extracts that were then analyzed using GC-MS. The GC-MS results showed that the isolates produced a variety of chemical compounds (Supplementary Figure 1 and Table 1). Three compounds were selected based on peak area dominance and reported biological activity in the literature: Compound 1 (cyclo(L-prolyl-L-valine)), Compound 2 (pyrrolo[1,2-a]pyrazine-1,4-dione,hexahydro-3-(2-methylpropyl)), and Compound 3 (2,5-piperazinedione, 3-methyl-6-(1-methylethyl)). These three compounds are commonly produced by Gram-positive bacteria, including the genus *Exiguobacterium*, as secondary metabolites with notable biological activities.

Molecular Docking Analysis of Designed Compounds

Molecular docking analysis of three bacterial-derived compounds against the EGFR active site (PDB ID: 1M17) revealed notable differences in binding performance compared to the native ligand erlotinib/AQ4. Among the tested compounds, compound 2 (pyrrolo[1,2-a]pyrazine-1,4-dione, hexahydro-3-(2-methylpropyl)) exhibited the strongest binding affinity, surpassing the native ligand, indicating its favorable interaction within the EGFR ATP-binding pocket (Table 3).

Despite forming fewer hydrogen bonds, compounds 2 (pyrrolo [1,2-a] pyrazine-1,4-dione, hexahydro-3-(2-methylpropyl)) demonstrated a stable binding conformation primarily driven by extensive hydrophobic and Van der Waals interactions, suggesting that overall binding stability was influenced more by interaction geometry and pocket complementarity than by hydrogen bond

Print ISSN: 2527-4384, Online ISSN: 2527-3442
DOI: 10.21705/mcbs.v10n1.751

Table 1. Results of colony and cell morphology observations.

Isolate	Colony Morphology				Cell Morphology		
	Shape	Elevation	Edge	Color	Shape	Gram	Endospore
B-1	Circular	Raised	Entire	Beige	Long bacil	Positive	+
B-2	Circular	Convex	Entire	Beige	Short bacil	Negative	-
B-3	Circular	Raised	Entire	Beige	Long bacil	Positive	+
B-4	Circular	Convex	Entire	Beige	Short bacil	Negative	-
B-5	Circular	Convex	Entire	Beige	Short bacil	Negative	-
B-6	Irregular	Flat	Curled	Beige	Short bacil	Positive	-

number alone. In contrast, compound 1 (Cyclo(L-prolyl-L-valine)) and compound 3 (2,5-piperazinedione,3-methyl-6-(1-methylethyl)), although forming multiple hydrogen bonds, showed comparatively weaker binding affinities, highlighting that a higher number of hydrogen bonds does not necessarily correlate with stronger binding. The native ligand erlotinib displayed a binding mode dominated by hydrophobic interactions, consistent with its established inhibitory mechanism (Figure 2).

The three test compounds occupied the active site of the EGFR tyrosine kinase domain, which is also the binding site for the control ligand AQ4, as shown by the three-dimensional visualization of the docking results. Compound 2 (pyrrolo [1,2-a] pyrazine-1,4-dione, hexahydro-3-(2-methylpropyl)), which had the highest affinity, occupied the deepest position in the active pocket and formed stable hydrophobic interactions, as shown in the three-dimensional image. Meanwhile, compounds 1 (Cyclo(L-prolyl-L-valine)) and 3 (2,5-piperazinedione,3-methyl-6-(1-methylethyl)) were also located within the active pocket, but with a slightly more open ligand orientation. The congruence in binding positions of these three compounds with the control ligand lent credence to the hypothesis that all three functioned as EGFR inhibitors by impeding kinase activity through competition with adenosine triphosphate (ATP).

Docking analysis against caspase-3 (PDB ID: 1PAU) demonstrated that all three bacterial-derived compounds exhibited stronger binding affinities than the native ligand Ac-DEVD-CHO (Table 4). Among them, compound 2 showed the most favorable docking score, indicating a higher binding propensity toward the caspase-3 structure. Notably, the binding poses of the tested compounds differed from that of the native ligand, which is known to occupy the catalytic active site of caspase-3. Visualization analysis revealed that the screened compounds interacted with alternative regions of the protein rather than the canonical substrate-binding pocket. This distinct binding

Table 2. Phenotypic characteristics of bacterial strains.

Characteristics	B-1 & B-3	B-2, B-4, B-5	B-6
Gram staining	+	-	+
Endospore formation	+	-	-
Biochemical tests			
Motility	+	+	+
Indol	-	-	-
H_2S (Hydrogen Sulfide)	+	+	-
Sugar	+	+	+
Gas	-	-	-
Methyl red (MR)	+	+	+
Voges proskauer (VP)	+	+	+
Citrate	+	+	-
Catalase	+	+	+

Table 3. Molecular docking results of test compounds and native ligand against EGFR (PDB ID: 1M17).

Compound	Mean±SD (kcal/mol)	Best Pose	RMSD	H Bond Interaction	Other Interactions
Cyclo (L-prolyl-L-valine)	–6,37±0,06	-6.4	0	Thr830, Thr766	Van der waals: Asp831, Glu738, Ile720 Alkyl: Val702, Leu820, Ala719, Leu764, Lys721, Met742
Pyrrolo[1,2-a]pyrazine-1,4-dione,hexahydro-3-(2-methylpropyl)	–7,13±0,12	-7.2	0	Thr830	Van der waals: Glu738, Thr766 Alkyl: Ala719, Leu820, Val702, Met742, Lys721, Leu764
2,5-piperazinedione,3-methyl-6-(1-methylethyl)	–5,87±0,06	-5.9	0	Thr830, Thr766	Van der waals: Asp831, Ala719, Ile720 Alkyl: Leu820, Val702, Met742, Leu764, Lys721(alkyl)
Ligand native: AQ4/erlotinib	–6,10±0	-6.1	0	Met769	Van der waals: Leu768, Pro770, Leu694, Gly772, Cys773, Phe771, Asp776, Met742, Thr766, thr830, lys721, leu820, val702, ala719

Table 4. Molecular docking results of test compounds and native ligand against caspase-3 (PDB ID: 1PAU).

Compound	Mean±SD (kcal/mol)	Best Pose (kcal/mol)	RMSD	H Bond Interaction	Other interactions
Cyclo(L-prolyl-L-valine)	–4,50±0,10	-4.6	0	-	Van der waals: Phe381D, Asp502, Ser381C, Phe381B, Trp340, Phe381H, Glu503 Alkyl: Val504
Pyrrolo[1,2-a]pyrazine-1,4-dione,hexahydro-3-(2-methylpropyl)	–5,97±0,06	-6.0	0	Tyr331	Van der waals: Met393, thr262, Leu258 Alkyl: Val390, Lys259 Pi-sigma: Tyr329
2,5-piperazinedione,3-methyl-6-(1-methylethyl)	–4,43±0,12	-4.5	0	Asp502, Trp348	Van der waals: Asn342, Phe381B, Glu381, Glu379A, Ser381A Pi-alkyl: Phe380
Ligand native: Ac-DEVD-CHO	–3,57±0,06	-3.6	0	His174, Met176, Phe173, Ser178	Van der waals: Asn172, Thr177, Lys175, Gly175C, Thr175B

behavior suggests that the identified compounds may act as potential allosteric modulators of caspase-3, possibly influencing its activity through a non-competitive mechanism (Figure 3).

Print ISSN: 2527-4384, Online ISSN: 2527-3442
DOI: 10.21705/mcbs.v10n1.751

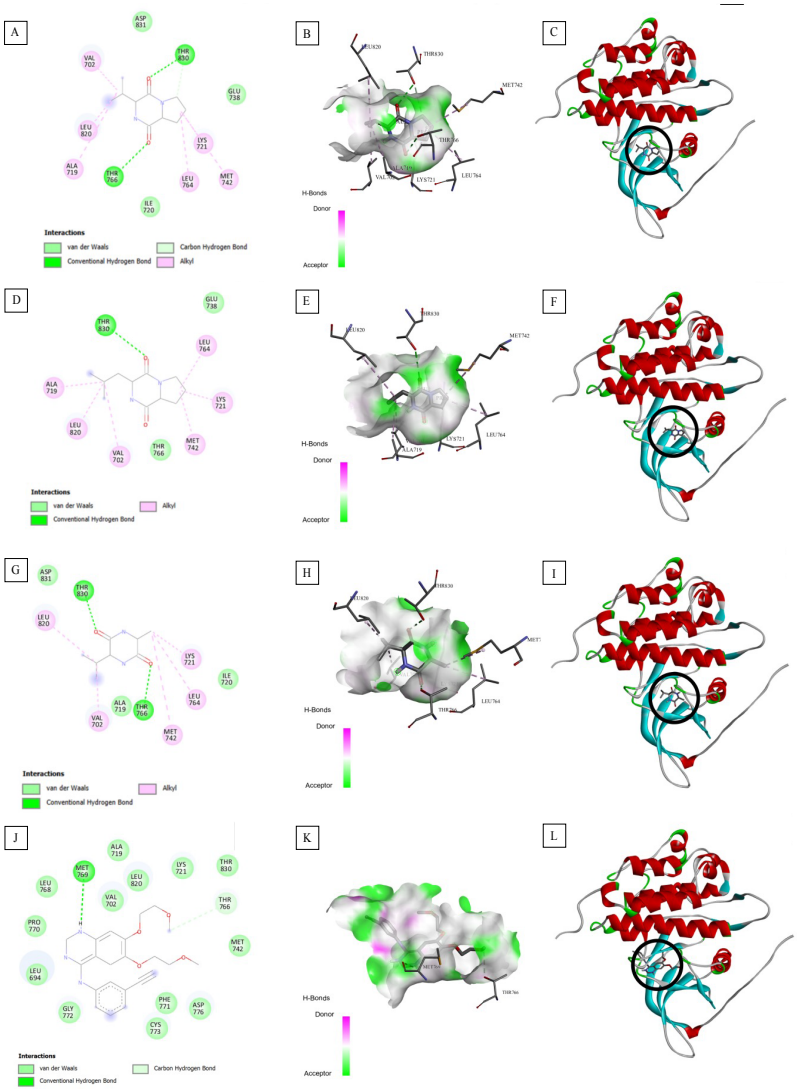

Figure 2. Molecular docking interaction analysis of compounds 1–3 and the native ligand AQ4 with the EGFR receptor (PDB ID: 1M17). For each ligand, panels show 2D interaction diagrams, surface interaction representations, and 3D binding poses within the EGFR active site. A, B, C: correspond to compound 1 (Cyclo(L-prolyl-L-valine)). D, E, F: compound 2 (pyrrolo [1,2-a] pyrazine-1,4-dione,hexahydro-3-(2-methylpropyl)). G, H, I: Compound 3 (2,5-piperazinedione,3-methyl-6-(1-methylethyl)). J, K, L: to the original AQ4 ligand.

In silico ADME Toxicity Prediction

In the initial screening stage of compounds from bacterial isolates, in-silico ADME assessment was used to predict pharmacological properties prior to in vitro and in vivo studies. The physicochemical parameters anticipated for compound (1) Cyclo(L-prolyl-L-valine), (2) pyrrolo[1,2-a] pyrazine-1,4-dione,hexahydro-3-(2-methylpropyl), and compound (3) 2,5-piperazinedione,3-methyl-6-(1-methylethyl) were calculated using SwissADME (http://www.swissadme.ch/). All three of the isolated compounds complied with Lipinski's rules, indicating their potential as oral drug candidates. Their cLogP values (<5), molecular weights (<500 g/mol), and TPSAs (below 140Å²) indicated physicochemical properties that supported absorption through biological membranes. Additionally, the identical bioavailability value of 0.55 for all three compounds suggested moderate oral absorption potential (Table 5). LD_{50} refers to the degree of acute toxicity of a xenobiotic and corresponds to the dose likely to kill 50% of the animals in the batch used for the experiment. In terms of toxicity, compounds 1 (Cyclo(L-prolyl-L-valine)) and 2 (pyrrolo[1,2-a]pyrazine-1,4-dione,hexahydro-3-(2-methylpropyl)) had an LD50 of 800 mg/kg, while compound 3 (2,5-piperazinedione,3-methyl-6-(1-methylethyl)) had a higher value of 1,000 mg/kg. All of these values fell into the low toxicity category (Class 4) (Table 5). Overall, compound 2 (pyrrolo[1,2-a]pyrazine-1,4-dione,hexahydro-

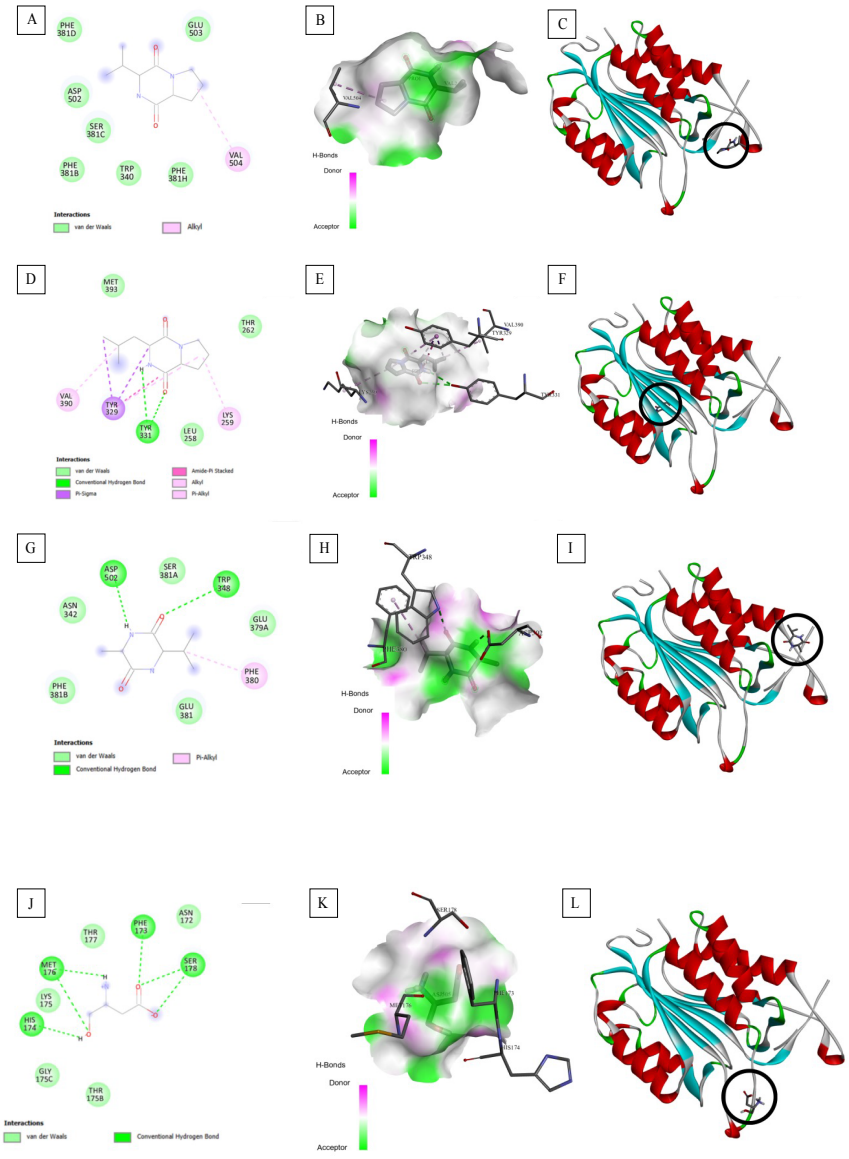

Figure 3. Molecular docking interaction analysis of Compounds 1–3 and the native ligand Ac-DEVD-CHO with the caspase-3 receptor (PDB ID: 1PAU). For each ligand, panels show 2D interaction diagrams, surface interaction representations, and 3D binding poses within the caspase-3 structure. A, B, C: correspond to compound 1 (Cyclo(L-prolyl-L-valine)). D, E, F: compound 2 (pyrrolo[1,2-a]pyrazine-1,4-dione, hexahydro-3-(2-methylpropyl)). G, H, I: compound 3 (2,5-piperazinedione, 3-methyl-6-(1-methylethyl)). J, K. L: to the native ligand Ac-DEVD-CHO.

3-(2-methylpropyl)) continued to demonstrate the best performance in terms of pharmacokinetics and toxicology, supporting its potential as a viable candidate for anticancer development.

Identification of Anticancer Compound Producing Bacterial Isolate through 16S rRNA Gene-based Sequencing Analysis

Molecular identification was performed by targeting the 16S rRNA gene. This is a conservative marker in bacteria. The gene was amplified using PCR, and the results were analyzed through sequencing. The nucleotide sequences obtained were then compared with the NCBI database using BLAST to determine the species identity of the isolate.[25] The results of DNA electrophoresis visualization of the bacterial isolate are shown (Figure 4).

The closest phylogenetic relatives of the isolate, as determined by 16S rRNA sequence similarity analysis (Table 6). The obtained sequences were aligned and analyzed in comparison to the GenBank database. BLAST searches revealed that the bacterial isolates were 98% identical to the *Exiguobacterium* genus (*Exiguobacterium* sp., *E.*

Print ISSN: 2527-4384, Online ISSN: 2527-3442
DOI: 10.21705/mcbs.v10n1.751

Table 5. Predicted ADME properties, oral bioavailability, and toxicity of compounds from bacterial isolates.

Ligand	ADME Proporties					Lipinski Rule of Five*	Bio-availability	LD (mg/kg)**
	H don [(a)]	H Acc [(b)]	cLogP	MW (g/mol)	TPSA			
Cyclo(L-prolyl-L-valine)	1	4	0.64	196.25	49.41	0	0.55	800 [(d)]
Pyrrolo[1,2-a]pyrazine-1,4-dione,hexahydro-3-(2-methylpropyl)	1	4	0.96	210.27	49.41	0	0.55	800 [(d)]
2,5-piperazinedione,3-methyl-6-(1-methylethyl)	2	4	0.22	170.21	58.20	0	0.55	1000 [(d)]

(a) Hydrogen bond donor

(b) Hydrogen bond acceptor

* Lipinski rule of five H donor<5, H acceptor<10, MW<500mg/ml, ClogP 2<5, TPSA<140 A°

** Lethal dose (LD) represent the acute toxicity, (d) toxicity level 4

acetylicum, *Exiguobacterium* sp. IARI-R-140, E. sp. CP-2, and *E. indicum*). According to CLSI recommendations for establishing taxonomic relationships between prokaryotic strains and bacterial categorization through DNA target sequencing, if the 16S rRNA sequence was 99% identical or higher, the strain was almost certainly the same species, while 97–98% similarity was used to identify organisms at the genus level.[26]

Discussion

Previous studies have reported various bacterial species in the Maros-Pangkep Karst area, including *Actinomycetes*.[8] However, no research has specifically identified *Exiguobacterium* from this region or explored its bioactive compounds. This study successfully isolated *Exiguobacterium* from soil beneath stalagmites in the Maros-Pangkep Karst and suggests its potential relevance as a source of bioactive compounds associated with anticancer properties. The isolate B-6 showed 98.11% similarity to members of the genus *Exiguobacterium* (Max Score=2207; E-value=0.0), indicating a close relationship but not sufficient for species-level assignment due to high sequence conservation among *Exiguobacterium* strains. *Exiguobacterium* are reported to harbor biosynthetic gene clusters potentially responsible for antimicrobial and anticancer metabolites, suggesting that the isolate may produce bioactive compounds. Previous reports also highlighted the anticancer potential of the *Exiguobacterium* genus through the production of bioactive compounds.[27-28] Three anticancer compounds were obtained from GC-MS results, namely compound (1) Cyclo(L-prolyl-L-valine) was reported to have anticancer properties and induce cell death in HeLa cells.[29] Pyrrolo[1,2-a]pyrazine-1,4-dione, hexahydro-3-(2-methylpropyl) was reported to exhibit cytotoxic activity against lung (A549) and cervical (HeLa) cancer cells through apoptosis.[30] Meanwhile, the compound 2,5-Piperazinedione, 3-methyl-6-(1-methylethyl) was studied as a procaspase 3 activator, while other reports indicate that derivatives of this compound can induce apoptosis in A549 and HeLa cancer cells.[31-32]

Docking analysis showed that the three *Exiguobacterium*-derived compounds occupied the tyrosine kinase domain of EGFR at the same binding site as the control ligand AQ4, indicating a potential competitive inhibition mechanism.[27,33] Compound 2 (pyrrolo[1,2-a]

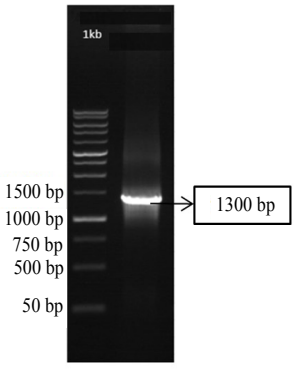

Figure 4. Visualization of bacterial B-6 DNA amplified using the 16S rRNA gene.

pyrazine-1,4-dione,hexahydro-3-(2-methylpropyl)) had the lowest docking score (–7.2 kcal/mol), showing the strongest binding affinity among the test compounds, even though it only formed one standard hydrogen bond with the Thr830 residue. This reinforces that the number of hydrogen bonds is not always the primary determinant of affinity, as contributions from van der Waals interactions, structural rigidity, and molecular polarity also play significant roles.[34] These results are consistent with previous studies that AQ4 binds to the ATP-binding pocket of EGFR involving key residues such as ARG-310, GLY-304, and TYR-300, thereby inhibiting kinase activity.[33] This supports that fourth-generation EGFR inhibitors act by competing with ATP, blocking phosphorylation, and suppressing cell proliferation.[35]

In contrast, docking analysis of caspase-3 revealed that the screened compounds interacted with regions distinct from the canonical binding site of the native ligand Ac-DEVD-CHO, suggesting a potential allosteric binding mode. The observed binding poses indicate that these compounds may function as allosteric modulators of caspase-3, although the specific functional outcome whether inhibitory or activating cannot be determined based solely on docking results. Such allosteric interactions may induce conformational changes that influence enzyme activity through a non-competitive mechanism.[36] This interpretation is supported by previous studies reporting the presence of regulatory allosteric sites in caspases that can modulate enzymatic function upon small-molecule binding. Previous structural studies have identified allosteric networks in caspase-3 in which binding at distal sites or mutations within the allosteric interface can alter enzyme activity by shifting the conformational ensemble between active and inactive states, supporting the concept that ligands binding outside the canonical active site may modulate caspase-3 behavior.[36-37]

Although the three compounds were evaluated individually, their distinct binding behaviors suggest that combination strategies may result in additive or synergistic effects, which warrants further investigation in future experimental studies. The computational predictions obtained in this study are consistent with previous reports highlighting microbial-derived small molecules, including cyclic dipeptides and diketopiperazine derivatives, as promising anticancer agents capable of modulating key

Table 6. Closest phylogenetic relatives of the bacterial isolate as determined by 16S rRNA gene sequence.

Isolate	Max Score	Close Relative	Identity %	E-value	Gene Bank Accession No.
B-6	2207	*Exiguobacterium* sp.	98.11	0	MK414878.1
	2207	*Exiguobacterium acetylicum*	98.11	0	MW041269.1
	2207	*Exiguobacterium* sp. IARI-R-140	98.11	0	JX429020.1
	2207	*Exiguobacterium* sp. CP-2	98.11	0	JN642681.1
	2207	*Exiguobacterium indicum*	98.11	0	LC873072.1

Print ISSN: 2527-4384, Online ISSN: 2527-3442
DOI: 10.21705/mcbs.v10n1.751

pathways involved in cell proliferation and apoptosis.[38] Importantly, the observed dual-target interaction with both EGFR and caspase-3 suggests a complementary biological effect, whereby inhibition of proliferative signaling may be coupled with modulation of apoptotic pathways.All three of the isolated compounds complied with Lipinski's rules, indicating their potential as oral drug candidates. The Rule of Five (Ro5), introduced by Lipinski et al., has become a widely accepted standard for assessing drug likeness and ADME. This rule states that potential oral drug candidates typically have a molecular weight of ≤ 500 g/mol. They also have ≤ 5 hydrogen bond donors. In addition, they have ≤ 10 hydrogen bond acceptors. Finally, they have cLogP ≤ 5. The LD50 value is an important parameter for classifying the toxicity of a compound. The online Protox-II web server predicted the acute oral toxicity LD50 (mg/kg) for mice.[39] In terms of toxicity, compounds 1 (Cyclo(L-prolyl-L-valine)) and 2 (pyrrolo[1,2-a]pyrazine-1,4-dione,hexahydro-3-(2-methylpropyl)) had an LD50 of 800 mg/kg, while compound 3 (2,5-piperazinedione,3-methyl-6-(1-methylethyl)) had a higher value of 1,000 mg/kg. All of these values fell into the low toxicity category (Class 4).

This study has several limitations. The anticancer potential of the identified metabolites was evaluated solely using in silico approaches, including molecular docking and ADME analysis, which require further validation through in vitro and in vivo experiments. In addition, the proposed allosteric modulation of caspase-3 is inferred from docking poses rather than direct functional evidence. Finally, the analysis was limited to a single *Exiguobacterium* isolate, and broader screening of isolates may provide more comprehensive insights.

Conclusion

This study identified three major secondary metabolites from a karst-associated *Exiguobacterium* isolate and evaluated their anticancer potential using in silico approaches. Among them, pyrrolo[1,2-a]pyrazine-1,4-dione, hexahydro-3-(2-methylpropyl) showed the strongest binding affinity toward EGFR, while all compounds exhibited potential allosteric interactions with caspase-3. Overall, this study highlights the potential of *Exiguobacterium* from the Maros-Pangkep Karst as a novel source of bioactive compounds with unique anticancer mechanisms and warranting further experimental validation.

Acknowledgments

The authors would like to express their gratitude for the support provided by the Department of Biology, Faculty of Mathematics and Natural Sciences, Hasanuddin University.

Authors' Contributions

The study concept was developed by TW, NH, HW, RW, and FG, while the study design was prepared by TW and HW. Supervision was provided by NH. Resources were supplied by NH and HW, and materials were contributed by HW, RW, and FG. Data collection and/or processing were performed by TW, NH, HW, and FG, whereas data analysis and/or interpretation were conducted by RW, TW, and HW. The literature search was carried out by TW, NH, HW, and FG. Manuscript writing was undertaken by TW, NH, and H.W., and critical review of the manuscript involved TW, NH, HW, RW, and FG. All authors agree to be accountable for all aspects of this work.

Ethical Statement

This study did not involve human participants, human biological materials, personal data, or live animals. Therefore, ethical approval from an institutional review board or ethics committee was not required.

Conflict of Interest

The authors declare that they have no conflicts of interest or competing interests related to the content of this manuscript.

References

1. Mane M, Yadav, S. In silico investigation of novel sorafenib analogues as potential inhibitors of VEGFR kinase and c-RAF kinase. J Res Pharm. 2024; 28(6): 2017-26.
2. Zubair T, Bandyopadhyay D. Small molecule EGFR inhibitors as anti-cancer agents: discovery, mechanisms of action, and opportunities. Int. J. Mol. Sci. 2023; 24: 1-19.
3. Hu L, Fan M, Shi S, Song X, Wang F, He H, *et al*. Dual target inhibitors based on EGFR: promising anticancer agents for the treatment of cancers. Eur. J. Med. Chem. 2022; 227: 1-18.
4. Mustafa M, Ahmad R, Tantry IQ, Ahmad W, Siddiqui S, Alam M, et al. Apoptosis: a comprehensive overview of signaling pathways, morphological changes, and physiological significance and therapeutic implications. Cells. 2024; 13(22): 1-29.
5. Pandey S, Jain S, Sahu SK, Gurjar VK, Vaidya A. Chapter 5 - caspase-3: a promising target for anticancer agents. Academic Press. 2024: 73-104. doi: 10.1016/B978-0-443-15644-1.00005-5.

6. Wijaya T, Akmal AAM, Herman N, Hasan AA, Hafiz A, Widyastuti H. Apoptotic effects sulfated polysaccharides of caulerpa racemosa extract on colorectal cancer cells through caspase-3. Mol Cell Biomed Sci. 2025; 9(3): 171-78.
7. Haedar N, iqram M, Ambeng, Yusriana, Priosambodo D, Lebe R. Bacterial communities on degraded prehistoric rock paintings in maros-pangkep global geopark. Phil J Sci. 2024; 153(1): 391-402.
8. Rante H, Manggau MA, Alam G, Pakki E, Erviani AE, Hafidah N, *et al*. Isolation and identification of actinomycetes with antifungal activity from karts ecosystem in Maros-Pangkep, Indonesia. Biodivers. 2024; 25(2): 458-64.
9. Desena FM, Ceferino NDIC, Cornelio SG, Villagomez CA, Candelario JLH, García SDIR. Bacteria halotolerant from Karst Sinkholes as a source of biosurfactants and bioemulsifiers. Microorganisms. 2022; 10(7): 1-18.
10. Li H, Li L, Chi Y, Tian Q, Zhou T, Han C, *et al*. Development of a standardized Gram stain procedure for bacteria and inflammatory cells using an automated staining instrument. Microbiologyopen. 2020; 9(9): 1-20.
11. Syafitri A, Fitri L, Suhartono S. Endophytic Bacteria in Acalypha indica L. Leaves and their antimicrobial activity against Staphylococcus aureus and Candida albicans. Mol Cell Biomed Sci. 2025; 9(2): 82-90.
12. Yang Z, Helmann T, Baudin M, Schreiber KJ, Bao Z, Stodghill P, *et al*. Genome-wide identification of novel flagellar motility genes in Pseudomonas syringae pv. Tomato DC3000. Front Microbiol. 2025; 16: 1-16.
13. Pardosi L, Manalu AI, Lisnahan CV. Isolation and characterization of superior symbiotic bacterial isolates from the Oenggae Sea with potential as antibacterial. J Biol Sci. 2024; 24(3): 403-11.
14. Chai B, Qiao Y, Wang H, Zhang X, Wang J, Wang C, *et al*. Identification of YfiH and the catalase CatA as polyphenol oxidases of Aeromonas media and CatA as a regulator of pigmentation by its peroxyl radical scavenging capacity. Front Microbiol. 2017; 8: 1-12.
15. Rammali S, Kamal FZ, El Aalaoui M, Bencharki B, Burlui V, Khattabi A, *et al*. In vitro antimicrobial and antioxidant activities of bioactive compounds extracted from Streptomyces africanus strain E2 isolated from Moroccan soil. Sci Rep. 2024; 14: 1-20.
16. Swamy MK, Sinniah UR, Akhtar MS. In Vitro Pharmacological activities and GC-MS analysis of different solvent extracts of Lantana camara leaves collected from tropical region of Malaysia. Evid Based Complement Alternat Med. 2015; 2015: 1-9.
17. Wardhani R, Darsih C, Iwansyah AC, Indriati A, Hamid HA, Husain DR. In Silico molecular docking approach and in vitro antioxidant and antimicrobial activity of Physalis angulata L. Extract. J Comput Biophys Chem. 2024; 23(2): 161-74.
18. Husain DR, Wardhani R. Antibacterial activity of endosymbiotic bacterial compound from Pheretima sp. earthworms inhibit the growth of Salmonella typhi and Staphylococcus aureus: in vitro and in silico approach. Iran J Microbiol. 2021; 13(4): 537-43.
19. Ayodele PF, Bamigbade AT, Bamigbade OO, Adeniyi IA, Tachin ES, Seweje Aj, et al. Illustrated procedure to perform molecular docking using PyRx and biovia discovery studio visualizer: a case study of 10kt with atropine. Prog Drug Discov Biomed Sci. 2023; 6(1): 1-31.
20. Nurjanah D, Fadilah, Dharmayanti NLPI. Virtual screening of indonesian herbal compounds with neuraminidase inhibitor activity against N2 influenza virus protein: an in silico study. Mol Cell Biomed Sci. 2024; 8(2): 105-16.
21. Dobrut A, Siemińska I, Sroka-Oleksiak A, Drozdz K, Sobonska J, Mroczkowska U, *et al*. Molecular and phenotypic identification of bacterial species isolated from cows with mastitis from three regions of Poland. BMC Vet Res. 2024; 20: 1-14.
22. Baer M, Höppe L, Seel W, Lipski A. Impact of DNA extraction, PCR amplification, sequencing, and bioinformatic analysis on food-associated mock communities using PacBio long-read amplicon sequencing. BMC Microbiol. 2024; 24: 1-17.
23. Baindara P, Mandal SM. Bacteria and bacterial anticancer agents as a promising alternative for cancer therapeutics. Biochimie. 2020; 177: 164-89.
24. Smibert RM, Kreig NR. Methods for General and Molecular Bacteriology. Washington DC: ASM Press; 1994.
25. Irshaid FI, Eshawakh SR, Hunaiti A, Al-Masri HT. Aromatic phosphinous amides: a promising new generation of antibiotics for = multidrug-resistant bacterial Infections. J Res Pharm. 2024; 28(5): 1800-11.
26. Lewis JS, Weinstein MP, Bobenchik AM, Campeau S, Cullen SK, Galas MF, *et al*. Performance Standards for Antimicrobial Susceptibility Testing. 32nd ed. Wayne: Clinical and Laboratory Standards Institute; 2022.
27. Jinendiran S, Teng W, Dahms HU, Liu W, Ponnusamy VK, Chiu CC, *et al*. Induction of mitochondria-mediated apoptosis and suppression of tumor growth in zebrafish xenograft model by cyclic dipeptides identified from Exiguobacterium acetylicum. Sci Rep. 2020; 10(1): 1-17.
28. Bharath PG, Varalakshmi KN. Caspase mediated cytotoxicity of a yellow pigment produced by Exiguobacterium alkaliphilum on human cancer cell lines. J Pharm Pharmacogn Res. 2020; 8(1): 78–91.
29. Hernández-Padilla L, Vázquez-Rivera D, Sánchez-Briones LA, Díaz-Pérez AL, Moreno-Rodríguez J, Moreno-Eutimio MA, *et al*. The antiproliferative effect of Cyclodipeptides from Pseudomonas aeruginosa PAO1 on HeLa cells involves inhibition of phosphorylation of Akt and S6k kinases. Molecules. 2017; 22(6): 1-18.
30. Lalitha P, Veena V, Vidhyapriya P, Lakshmi P, Krishna R, Sakthivel N. Anticancer potential of pyrrole (1, 2, a) pyrazine 1, 4, dione, hexahydro 3-(2-methyl propyl) (PPDHMP) extracted from a new marine bacterium, Staphylococcus sp. strain MB30. Apoptosis. 2016; 21(5): 566-77.
31. Yanuar A, Pratiwi I, Syahdi RR. In silico activity analysis of saponins and 2, 5-piperazinedione from marine organism against murine double minute-2 inhibitor and procaspase-3 activator. J Young Pharm. 2018; 10(2): 16-19.
32. Li X, Xun T, Xu H, Pang X, Yang B, Wang J, *et al*. Design, synthesis, and anticancer activity of novel 3,6 Diunsaturated 2,5 Diketopiperazines. Mar Drugs. 2023; 21(6): 1-19.
33. Dera AA, Al-Fayi M. CEG-0598, a novel dual inhibitor of EGFR and C5aR demonstrates in vitro anticancer and antimetastatic activity in prostate cancer cells. Discov Onc. 2025; 16: 1-20.
34. Chen D, Oezguen N, Urvil P, Ferguson C, Dann SM, Savidge TC. Regulation of protein-ligand binding affinity by hydrogen bond pairing. Sci Adv. 2016; 2(3): 1-9.
35. Tariq A, Shoaib M, Qu L, Shoukat S, Nan X, Song J. Exploring 4th generation EGFR inhibitors: a review of clinical outcomes and structural binding insights. Eur J Pharmacol. 2025; 997: 175-86.
36. Scheer JM, Romanowski MJ, Wells JA. A common allosteric site and mechanism in caspases. Proc Natl Acad Sci USA. 2006; 103(20): 7595-600.
37. Cade C, Swartz P, MacKenzie SH, Clark AC. Modifying caspase-3

Print ISSN: 2527-4384, Online ISSN: 2527-3442
DOI: 10.21705/mcbs.v10n1.751

activity by altering allosteric networks. Biochem. 2014; 53(48): 7582-95.

38. Sukmarini L. Natural Bioactive cyclopeptides from microbes as promising anticancer drug leads: a mini-review. Indones J Pharm. 2021; 32(3): 291-303.

39. Bunally SB, Luscombe CN, Young RJ. Using physicochemical measurements to influence better compound design. SLAS Disc. 2019; 24(8): 791-801.